Application of global stability approaches to whistling jets and wind instruments

D. Fabre[a], P. Bonnefis[a], F. Charru[a], S. Russo[b], V. Citro[b], F. Giannetti[b] and P. Luchini[b]
[a]IMFT, University of Toulouse, allée du Professeur Soula, 31400 Toulouse, France
[b]DIIN, Universita di Salerno, Fisciano, 84084 Salerno, Italy
david.fabre@imft.fr

We discuss the application of the so-called *global approaches*, arising from the field of hydrodynamical instabilities, to aeroacoustic resonators. We illustrate the potential of the approach for the case of a jet passing through two successive holes ("hole-tone" configuration) which is relevant to human whistling, birdcalls and tea kettles. First, treating the hydrodynamic system as locally incompressible and linearized around a base flow, we compute the conductivity of the double aperture and show that this one can provide positive energy feedback to an external system. Secondly, introducing the coupling with an acoustical resonator through convenient impedances imposed as boundary conditions and solving an eigenvalue problem, we show that the full system is effectively linearly unstable and able to support self-sustained oscillations. The results compare favorably with recent experiments, and the analysis yields novel insight into the nature of the feedback mechanism responsible for the whistling. The application to the related situation of a corrugated pipe, and to more realistic instruments such as ocarinas and free reeds, will also be discussed.

1 Introduction

Wind instruments, and most particularly those of the flute family, are in essence self-sustained oscillators composed of two parts : an acoustic system (the tube or more generally the resonator) and a hydrodynamic system (a shear flow such as a jet or a shear layer). The second system is essential for its ability to provide positive energy feedback to the first one, but is generally the less understood. The most common approaches to such problems are the so-called lumped models, in which the hydrodynamical system is reduced to a *discrete system* with a limited degrees of freedom arising from a crude modeling of the flow, which disregards important features such as the thickness of the boundary layers and shear layers, the role of viscosity, etc... The purpose of this work is to explore an alternative approach, which consists of treating the hydrodynamical system as a *continuous system* and to resolve it in a rigorous way starting from the full Navier-Stokes equations in a representative computational domain.

More specifically, our goal is to explore the potential of a range of modern theoretical/numerical methods called *global stability approaches*. Those methods are particularly suited to reproduce and explain the behaviour of hydrodynamic self-sustained oscillators, such as vortex shedding in the wake of bluff bodies [2], resonating cavities [3] or path oscillations of falling objects [4]. For such problems, the combination of linear, weakly nonlinear and sensitivity approaches allows to predict the thresholds of self-oscillation, the amplitudes of the limit cycles and to determine the effect of small structural perturbations on the flow field, and ideally complement heavier numerical approaches such as direct simulation.

For the application to aeroacoustic resonators, the key idea of our approach is to assume that the hydrodynamical system is *locally incompressible* (an hypothesis which is justified because the typical Mach numbers are low and because the acoustical wavelengths are generally larger than the dimensions of the hydrodynamical system) and model the interaction with the acoustic system through the imposition of complex impedances as boundary conditions of the hydrodynamic system.

After presenting the bases of the global stability approaches, we will illustrate their potential for the case of a jet passing through two successive holes ("hole-tone" configuration) which is relevant to human whistling, birdcalls and tea kettles. Application to the related situation of a corrugated pipe, and to more realistic instruments such as ocarinas and free reeds, will also be discussed.

2 Global approaches for hydrodynamic instabilities: brief introduction

We give here a brief introduction to the global methods, with the emphasis on the similarities and differences with respect to classical linearized approaches in acoustics.

The starting point for global hydrodynamical approaches is the assumption that the total flow field $[\mathbf{U}_{tot}, P_{tot}]$ only displays small-amplitude deviations $[\mathbf{u}, p]$ with respect to a mean state called the *base flow* $[\mathbf{U_0}, P_0]$. Namely :

$$[\mathbf{U}, P] = [\mathbf{U_0}, P_0] + \epsilon[\mathbf{u}, p]e^{-i\omega t} + \mathcal{O}(\epsilon^2) \tag{1}$$

with $\epsilon \ll 1$. The first step is the calculation of the base flow, namely a steady solution of the incompressible Navier-Stokes equations, which can be written in a formal way as follows :

$$NS([\mathbf{U_0}, P_0]) = 0 \tag{2}$$

This base flow is usually solved using iterative methods, such as the Newton-Raphson algorithm. We employ this numerical procedure because of it is extremely efficient due to its quadratic convergence property.

Then, assuming that the perturbation is of small amplitude[1], the perturbation obeys a linear system which can be written formally as follows :

$$\partial_t \mathbf{u} = -i\omega\mathbf{u} = \mathrm{NSL}(\mathbf{u}, p) \tag{3}$$

Where the operator NSL represents in a symbolic way the linearized Navier-Stokes equations. Starting from this linear system, we present briefly some possible analysis:

(i) Forced problem: Just as customarily done in linear acoustics, we can impose a non-homogeneous boundary condition (either on the pressure p or on the flow rate q) in the form of a harmonic forcing with frequency ω (real). After discretization, the linear system (2) gets the form $(\mathcal{A} - i\omega\mathcal{B})X = F$, where X is the discretized version of the unknown flow field $[u, p]$, $\mathcal{A}, \mathcal{B}$ are matricial operators, and F represents the forcing term. In open flows, this method can be used to characterize the ability of a shear flow to amplify spatially perturbations as consequence of a local forcing. We will show that the same method can also be used to characterize the possible retroaction of a shear flow in on a acoustic system.

[1] Note that in global stability approaches, the small amplitude condition amounts $\epsilon|\mathbf{u}| \ll |\mathbf{U}_0|$, which differs from the condition normally used in linear acoustics, namely $\epsilon|\mathbf{u}| \ll c_0$. Note also that our linear approach fully retains the interactions of velocity perturbations with the base flow, which are usually considered as a nonlinear effects in classical acoustics.

(*ii*) Eigenvalue calculation: we consider the linearized problem with homogeneous boundary conditions. After discretization, the problem gets the classical eigenvalue form: $(\mathcal{A} - i\omega\mathcal{B})X = 0$. Note that here, the eigenvalues $\omega = \omega_r + i\omega_i$ are generally complex numbers. The interesting situations are encountered when $\omega_i > 0$, in which case the flow is said to be *globally unstable*. The corresponding eigenvector X is called the *global mode.* Note that instability generally arises as a consequence of the mean flow shear $\nabla \mathbf{U}_0$; while viscosity generally has a stabilizing effect. So in most situations, global instability is encountered when the Reynolds number Re exceeds a threshold value Re_c.

(*iii*) Structural sensitivity: This third approach, which is a quite recent development in global stability theory [1, 2], provides the possibility to identify the spatial regions of the flow which are responsible of the self-sustained instability mechanism. This tool is based on the concept of *adjoint eigenmodes* $[\mathbf{u}^\dagger, p^\dagger]$. Mathematically, an adjoint mode corresponds to the solution of the transposed eigenvalue problem $(\mathcal{A}^T - i\omega\mathcal{B}^T)X^\dagger = 0$. Physically, it represents the local receptivity of the mode to external forcing. Another key quantity is the so-called *wavemaker*, defined mathematically as $\mathcal{WM} = |\mathbf{u}| \cdot |\mathbf{u}^\dagger|$. Physically, this quantity represents the local ability of the mode to provide positive feedback on itself, so it is a very powerful tool to identify the regions of the flow responsible for the instability mechanism.

(*iv*) Weakly nonlinear method: This methods consists of continuing the expansion (1) as a series of powers of ϵ. Then, solving up to third order and applying compatibility conditions yields amplitude equations. The latter allow to predict the properties of the limit cycle corresponding to self-sustained oscillations in the vicinity of the threshold of instability.

3 The "hole-tone" configuration

The " hole-tone" configuration consists of a circular jet exiting for a circular hole and going through a second hole of approximately the same radius in a plate positioned downstream. This situation gives rise to powerful whistling tones and is encountered in various situations, including human whistling, birdcalls, tea kettles, as well as many industrial appliances. First studied by Sondhaus [5], this situation has attracted interest of early acoustic researchers, including Helmholtz, Rayleigh [6], and Bouasse [7]. Recently, Henrywood & Agarwal [8] conducted a minutious experimental investigation and identified two regimes : at low velocities the frequency is selected by the cavity located between the two holes, while are high velocity it is selected by the jet dynamics. Yet, the mechanism allowing positive energy feedback in each of these regimes, and the detailed interplay between the acoustic and hydrodynamical system remains to be clarified.

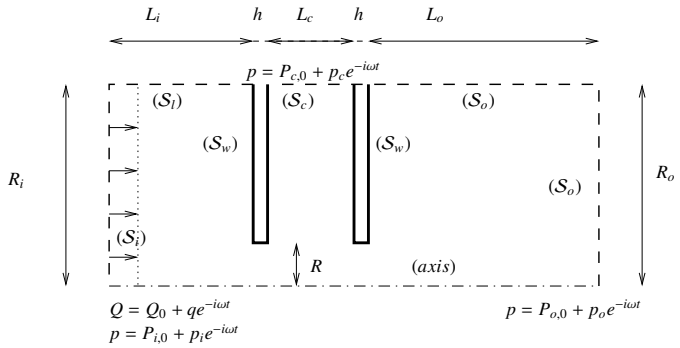

Figure 1: Geometry and computational domain for the tone-hole configuration

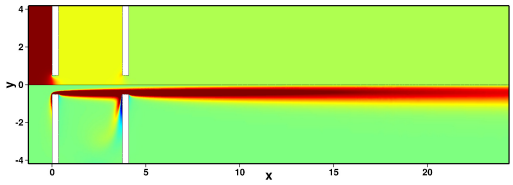

Figure 2: Structure of the incompressible base flow for $Re = 500$ (upper half : pressure ; lower half : vorticity).

3.1 Geometry and base flow

The geometry used for the global calculations is displayed in figure 1. The flow goes through two successive holes in plates of radius R and thickness h. The boundaries associated with the "walls" are noted $\mathcal{S}_w$, and the lateral boundary of the cavity enclosed between the two plates is noted $\mathcal{S}_c$. The computational domain includes an "inlet chamber" with boundaries $\mathcal{S}_i$ and $\mathcal{S}_l$ and an outer domain with boundary $\mathcal{S}_o$. He choose the dimensions of the holes and cavity to be geometrically similar with case (2) of ref. [8] ; namely, $R = 1/2, h = 1/3, L_c = 6.08, R_c = 4.1666$. The dimensions of the inlet chamber and outer domain are not important : they are taken sufficiently large so as not to influence the results.

The numerical discretization uses finite-elements relying on the FreeFem++ software. Thanks to the automatic mesh adaptation facility provided by this software, the numerical mesh is refined in the region of the shear layer, and especially at the edges of the holes where the flow displays the steeper gradients.

The base flow is computed as the steady solution with a constant volume flux Q_0. In practice we set this flow by imposing a constant normal velocity at the inlet boundary $\mathcal{S}_i$. We impose no-slip conditions ($\mathbf{U}_0 = 0$) on the walls $\mathcal{S}_w$, no-penetration condition ($\mathbf{U}_0 \cdot \mathbf{n} = 0$) on the lateral wall $\mathcal{S}_l$ of the inlet chamber, and convenient outlet conditions [4] on the outer boundary $\mathcal{S}_o$. The boundary of the intermediate cavity $\mathcal{S}_c$ is generally considered as closed, but the case of an open cavity has also been tried.

The base flow is parametrized by the Reynolds number based on the diameter and the mean velocity across the hole:

$$Re = \frac{2RU_m}{\nu} = \frac{2Q_0}{\pi R\nu} \tag{4}$$

The computed base flow is represented in figure 2 for the case $Re = 500$. The most important quantity associated to the base flow is the relationship between the flow rate U_m

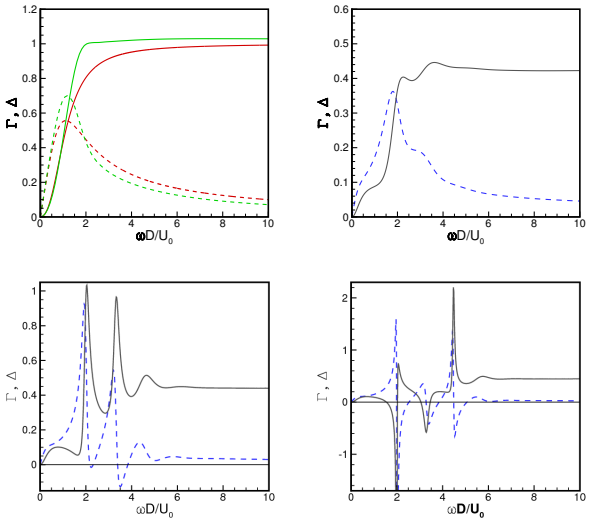

Figure 3: Real part Γ (plain lines) and imaginary part Δ (dashed lines) of the conductivity for (*a*) a single hole with $Re = 500$; (*b*) two holes with $Re = 100$; (*c*) two holes with $Re = 300$; (*d*) two holes with $Re = 500$. In (*a*) thinner lines correspond to inviscid theory [9].

and the pressure loss $P_{i,0} - P_{o,0}$. For the case displayed in the figure we obtain $(P_{i,0} - P_{o,0})/(\rho U_m^2) = 1.047$.

Although not displayed here, we have also considered for purposes of numerical validation the case of a jet passing through a single hole of zero thickness. In this latter case, for Re in the range $[500 - 1000]$ we find an almost constant value of the pressure drop, $(P_{i,0} - P_{o,0})/(\rho U_m^2) \approx 1.278$. This compares well with the classical modeling obtained from the Bernoulli theorem, which leads to $(P_{i,0} - P_{o,0})/(\rho U_m^2) = 1/(2\alpha^2)$, where $\alpha \approx 0.625$ is the so-called vena contracta coefficient [9].

3.2 Response to a harmonic forcing

Following method (*i*) described in section 2, the response to harmonic forcing is done by solving a linear system, where the right-hand-side represents the modulation of the flow rate along the inlet boundary (see figure 1). We first validated the approach for the case of a single hole where a theoretical model is available [9].

3.2.1 Theory : the Rayleigh-Howe conductivity

The problem of unsteady, low-amplitude flow though a circular aperture was initially solved by [6] in absence of a mean flow and in the potential case. The problem was reconsidered by [9] in the presence of a mean flow across the hole, modeled as a potential jet bounded by a circulation sheet. The key quantity in this situation is the conductivity, defined as the ratio between the fluid acceleration and the pressure jump across the aperture :

$$K \equiv 2R(\Gamma - i\Delta)\frac{-i\omega\rho_0 q}{(p_+ - p_-)}$$

Physically, the real part Γ corresponds to a reactance and can be related to the "equivalent length" of the plug of fluid oscillating back and forth through the hole, encountered in the classical theory of the Helmholtz resonator. The

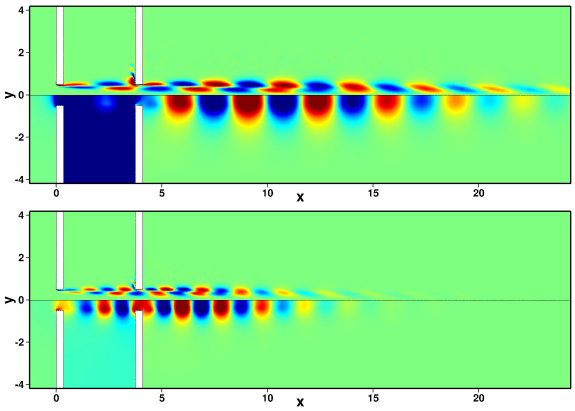

Figure 4: Flow perturbation due to a small-amplitude harmonic forcing for $\omega R/U_0 = 2$ (*a*) and $\omega R/U_0 = 3.3$ (*b*). Upper half : pressure ; lower half : vorticity.

imaginary part Δ correspond to a resistance. In the absence of mean flow, the classical result is $K = 2R$, hence $\Gamma = 1, \Delta = 0$. Howe [9] extended this result yielding formulas giving Γ and Δ in terms of the Strouhal number $St = \omega R/U$. These predictions are plotted in figure 3*a* with thin lines. Note the quantity Δ is directly related to the flux of energy transferred from the incoming oscillating flow to the jet (Eq. 4.6 of [9]). For a single hole Δ is always positive, meaning that the aperture acts as a sink of energy.

3.2.2 Numerical result : single hole configuration

The thick lines in the figure 3(*a*) display the two components of the conductivity computed through our approach, in the case $Re = 500$. The agreement with the prediction of [9] is quite good, especially in the low-frequency range. We have also repeated the calculation for other values of Re, and find that the results are almost independent of viscosity for $Re > 500$.

3.2.3 Numerical results : two-hole configuration

We now come back to the configuration with two successive holes. Figure 3 displays the computed conductivities, for $Re = 100, 300, 500$. We find that as Re is increased, Δ becomes negative in several intervals of frequencies. This means that the jet can actually act as a source for energy for the incoming flow. This is a strong indication of global instability of the hydrodynamical system.

Figure 4 shows the structure of the flow perturbation (depicted through pressure and vorticity isocontours), for two values of ω which corresponds to situations leading to negative Δ. It can be seen that the perturbation is characterized by an even number of vertical structures inside the cavity. On the other hand, for the values of ω corresponding to a maximum of Δ , the structure (not shown) is characterized by an odd number of structures. This suggest that the phase relationship between the vortex shedding process occurring at each holes plays a key role in the process.

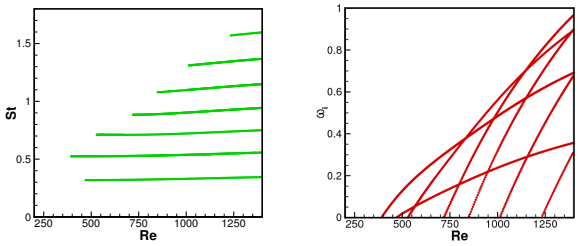

Figure 5: Strouhal number $St = \omega_r R/(2\pi U_0)$ and amplification rates ω_i of the global modes as function of Re in the case of a closed cavity.

3.3 Eigenvalue analysis

We thus revert to an eigenvalue calculation (approach (*ii*) of section 2) of the linearized hydrodynamical problem with homogeneous boundary conditions. Apart from the wall $\mathcal{S}_w$ where the no-slip, condition ($\mathbf{u} = 0$) is the only relevant one, we have to discuss the condition at surfaces $\mathcal{S}_i$ and $\mathcal{S}_o$ representing the matching with upsteam and downstream domain, and the condition at the "bottom" of the inlet cavity $\mathcal{S}_c$. As a starting point, we simply impose a vanishing of the oscillating pressure at the inlet and outlet : $p_i = p_o = 0$. Physically, this signifies that two-holes junctions actually separates two outer domains of very large volume, and that radiation losses are neglected. These assumptions could be improved in a subsequent step, for instance by using a reactive impedance modeling the effect of a large volume upstream and a resistance modeling the effect of radiation losses downstream, but we leave these issues aside and concentrate here on the modeling of the condition at the bottom of the cavity $\mathcal{S}_\rfloor$. We will consider two cases :

3.3.1 Results for a "closed cavity"

In the assumption of a closed cavity, $\mathcal{S}_\rfloor$ is considered as a rigid wall, so we use the no-slip condition condition $\mathbf{u} = 0$. Because of incompressibility, this also implies that the instantaneous flow rate q though both holes is the same.

We have solved the global stability problem for this case with Re ranging from 200 to 1400. The real and imaginary parts of computed eigenvalues are plotted as function of Re in plot 5. We can see that as $Re = Re_c \approx 400$ the flow becomes globally unstable, with the onset of a global mode with oscillation rate $\omega_r \approx 3.3$. Then as Re up to 6 other modes also gets unstable.

Figure 6(a) displays the structure of the unstable global mode obtained for $Re = 500$ (for a slightly different geometry where the edges of the hole are rounded). The structure is very similar to that obtained for the forced problem with ω (figure 4b). In addition, we also display the structure of the corresponding adjoint mode (figure 6(b)) and wavemaker (figure 6(c)). These quantities indicate that the instability mechanism entirely lies within the portion of the shear layer located inside the two cavities. Moreover, the highest level in both the adjoint and the wavemaker is encountered just at the edge of the first hole, at the point of formation of the shear layer.

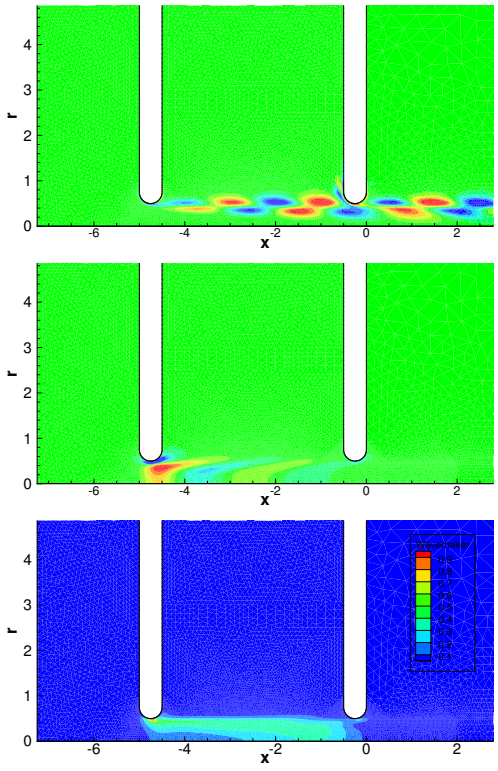

Figure 6: (a) Most unstable eigenmode for Re=500 (vorticity) ; (b) corresponding adjoint $u_x^\dagger$; (c) corresponding wavemaker.

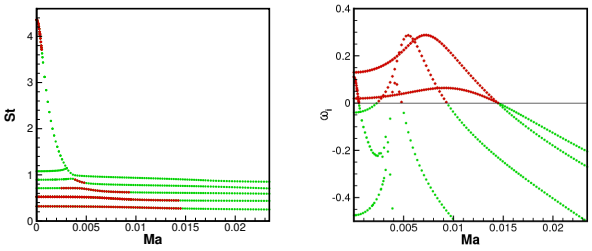

Figure 7: Strouhal number $St = \omega_r R/(2\pi U_0)$ and amplification rates ω_i of global modes as function of Mach, in the case of a "reactive" cavity

3.3.2 Results for a "reactive cavity"

According to [8], in the low-frequency range, the frequency is selected by the resonance of the cavity located between the two holes. To capture this régime, we have to introduce in our locally incompressible model an impedance representing the effect of compressibility inside the cavity. In the line of the classical modeling of the Helmholtz resonator, we write the balance of mass inside the cavity :

$$\frac{\partial(\rho' V_{cav})}{\partial t} = \frac{V_{cav}}{c_0^2}\frac{\partial p_{cav}}{\partial t} = \rho_0 q_{cav}, \tag{5}$$

Where q_{cav} is the volume flux coming out of the cavity. Expressed as an impedance, this leads to :

$$Z_{cav} = \frac{p_{cav}}{q_{cav}} = -\frac{\rho c_0^2}{i\omega V_{cav}}$$

To remain consistent with our locally incompressible assumption, we have to impose this volume flux at the upper

boundary of the computational domain representing the cavity. We emphasize that the actual volume of the cavities in the computed domain displayed in figure 1 does not need to be the same as the volume V_{res} of the assumed resonator. The procedure being, by essence, a asymptotic matching, the numerical volume is only required to be "sufficiently large" to allow a matching with a uniform pressure.

Note that the definition of the impedance of the cavity introduces the speed of sound c_0, which was absent from the purely incompressible case considered so far. Consequently, the problem is now characterized by two non dimensional parameters : $Re = RU_0/\nu$ and $Ma = U_0/c_0$. To compare with the experimental results of Henrywood & Agarwall, we have chosen to privilegiate a similitude in terms of the Mach number, and to fix arbitrarily the Reynolds to $Re = 500$ [2]. The eigenvalues of the global modes computed in this way are displayed as function of Ma in figure 7 (the branches are overlined in red on the portions of the curves corresponding to instability). The result clearly show the existence of the two kinds of branches and a switching between two regimes. The first series of branches have approximatively constant Strouhal numbers. Their structure (figure 8a) is qualitatively similar to those obtained in the closed case of through conductivity calculations. These modes are of hydrodynamical nature and weakly influenced by the effect of compressibility on the cavity. A branch of a different nature exists only in the low-mach range, and the corresponding Strouhal is inversely proportional to Ma. This means that the dimensional frequency is independent of the flow velocity going through the two apertures. This mode can be identified with the "Helmholtz" mode of the cavity. Indeed, inspection of its structure (figure 8b) shows that the flow rate going through each holes associated with the perturbation are in phase. The transition between the two regimes revealed by our results is in perfect agreement with the experimental observations of [8]. The difference is that we generally obtain several unstable global modes with different frequencies, while in the experiment a single frequency is observed. The selection between the several modes revealed by global stability calculations is most likely a nonlinear process.

4 Summary and perspectives

4.1 Summary for the tone-hole configuration

In this paper, we have illustrated the applicability of global stability approaches to aeroacoustic resonator, focussing mainly on the tone-hole generic configuration. We have shown that the results are in good accordance with experiments, and provide original insight into the physical mechanism responsible for self-oscillation. In particular, in the regime in which the frequency selection is of hydrodynamical nature (the high-velocity regime in figure 7), our result indicate that the compressibility of the flow does not play any role, contrary to the argument of [8] who suggest that the positive feedback is provided by emission of sound waves by the vortices formed at the second hole which propagate back towards the first hole.

[2] For higher Re, the results are qualitatively similar as for Strouhal numbers of the global modes; on the other hand the computations require much finer meshes

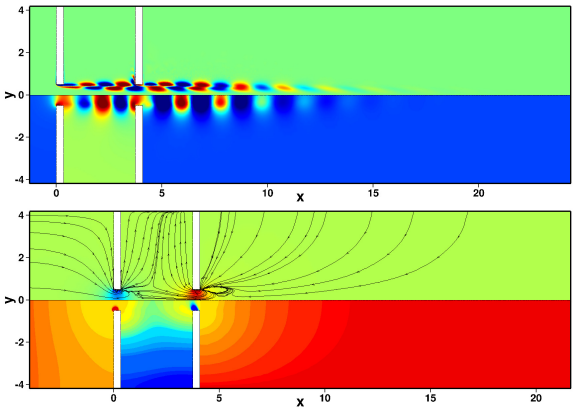

Figure 8: Structure of the global unstable modes in with a reactive cavity for (a) $Ma = 0.01$, $Re = 500$ and $St = 0.52$ ($\omega_r = 3.3$) ; and (b) $Ma = 0.001$, $Re = 500$ and $St = 8.3$ ($\omega_r = 26$). the two main regimes, in the case of a "reactive" cavity. In (b) the streamlines associated to the eigenmode are displayed.

4.2 Application to wind instruments

Motivated by this first success, our goal is now to apply the same approach to the modeling of wind instruments. A second successful attempt has already been done for the case of a whistling corrugated pipe[10], which, if not yet a "true" musical instrument, is able to generate several tones of musical interest. In this case, the global incompressible approach is able to describe the hydrodynamic instability mechanism which interacts with the standing waves of the tube to generate the tones. Our next step is to apply the same methods to flute-like instruments. In accordance with our general idea, which is to concentrate on the hydrodynamical part of the problem and to simplify as much as possible the acoustic part, an ocarina-like instrument, with a single frequency, would be the best candidate. Finally, we are currently exploring the applicability of the approach to reed instruments, especially free-reeds where the acoustic part is the simplest. The situation is certainly more difficult, but we expect to treat it also through a kind of "reactive" boundary condition representing the effect of displacement of the reed.

References

[1] P. Luchini, A. Bottaro; Ann Rev. Fluid Mech, Vol. 46: 493-517 (2014).

[2] F. Giannetti, P. Luchini; J. Fluid Mech. 581, p.167 (2007).

[3] D. Sipp, A. Lededev; J. Fluid Mech. 593, p.333 (2007)

[4] J. Tchoufag, D. Fabre, J. Magnaudet; J. Fluid Mech 770, p.278 (2014).

[5] C. Sonhauss, Annalen der physik 167-1 (1855).

[6] J. W. S. Rayleigh, The theory of sound (1945)

[7] H. Bouasse, Instruments à vent, Tome II (1930)

[8] R. H. Henrywood, A. Agarwal ; Phys. Fluids 25, 107101 (2013)

[9] M. S. Howe, Proc. R. Soc. Lond. A. 366, p.205 (1979)

[10] Nakiboglu, G., Rudenko, O., Hirschberg, A. (2012). J. Acoust. Soc. Am. 131(1), 749-765.